200. Electrostatic Deformation Properties in the Crystal Structure of Tricyclo[4.4.1.0^{1,6}]undeca-2,4,7,9-tetraene-11,11-dicarbonitrile

by **Riccardo Bianchi, Tullio Pilati** and **Massimo Simonetta***

Department of Physical Chemistry and Electrochemistry and C.N.R. Center, University of Milano, Via Golgi 19, I-20133 Milano

Dedicated to Prof. *J.D. Dunitz* on the occasion of his 60th birthday

(24.IV.84)

Summary

The deformation density and potential have been determined in molecular crystals of tricyclo[4.4.1.0^{1,6}]undeca-2,4,7,9-tetraene-11,11-dicarbonitrile at 150 K from X-ray diffraction measurements. A significant deformation density peak is found near the mid-point of the transannular bond. The four short bonds in the annulene ring acquire slightly more residual density compared to the other bonds, confirming the bisnorcaradienic character of the molecule. Similar trends are noted in the deformation electrostatic potential maps.

Introduction. – The present work is connected with the study of the equilibrium [10]annulene⇆bisnorcaradiene. The most interesting feature involved in the ring-closure reaction of 1,6-methane[10]annulene is the variation of the C(1)–C(6) transannular distance from 2.269(5) Å, found in 11,11-difluoro-1,6-methano[10]annulene [1], to 1.539(2) Å for tricyclo[4.4.1.0^{1,6}]undeca-2,4,7,9-tetraene-11,11-dicarbonitrile (DICN) [2]. So, the DICN molecule represents the last stage of the ring-closure reaction path for the parent hydrocarbon. The determination of the electrostatic deformation properties of DICN from X-ray diffraction data contributes to confirm and to get further insight about the chemical bond in this molecule.

Experimental. – Diffracted intensities were collected at 150 K on a *Enraf-Nonius CAD4* diffractometer equipped with a graphite monochromator (Mo$K\alpha$ radiation, $\lambda = 0.71069$ Å). DICN crystals are unstable at r.t. and they are orthorhombic, space group $P2_12_12_1$. A spherical crystal (radius 0.14 mm) was cooled by means of a N_2-stream, using the *Enraf-Nonius* gas-flow low-temperature device. Although the system is simple in handling, serious ice formation on the crystal occurred during data collection. This effect was minimized by interrupting the gas flow to allow the ice to melt, whenever it was necessary. The temperature of the cold N_2-stream was monitored during the experiment by means of a Cu-constantan thermocouple, which was placed in the cold gas tube. The temp. remained stable within 2 K. Two standard reflections were recorded every 120 min. The intensity fluctuations were less than about 4%. Peak profiles were measured with a continuous $\omega/2\theta$ step scan method. The scan range used during the measurements was taken according to the formula $\Delta\omega = 1° + 0.35°\text{tg}\theta$, in which $\Delta\omega$ is the scan range in θ. The final data set of 3363 reflections was collected in one octant with $2\theta < 80°$, and $\sigma(I)$ the standard deviation in I was estimated as $(P + B + 0.0002I^2)^{1/2}$ where P = integrated peak intensity, B = sum of background counts at each end scan, $I = P-B$. The average number of reflections measured per hour is 47.

Refinements. – 206 reflections with P < B and 37 imprecisely measured weak reflections were excluded from all refinements based on $|F(H)|^2$. The quantity minimized was $\Sigma_H w(H)\{|F_o(H)|^2 - k^2|F_c(H)|^2\}^2$ with $w(H) = 1/\sigma^2\{|F_o(H)|^2\}$. The data were corrected for isotropic extinction [3] as determined by least-squares ($y_{min} = 0.94$, $y = F^2_{obs}/F^2_{corr}$). A conventional refinement, based on the structure as reported by *Bianchi et al.* [2], converged rapidly.

Atomic scattering factors for C and N were calculated by the program *Valray* [4] using the *Hartree-Fock* wave function given by *Clementi* [5]. A single monopole scattering factor, computed by the program *Valray* [4] from *Slater* atomic orbital with fixed standard molecular exponent α [6], was assigned to each H-atom.

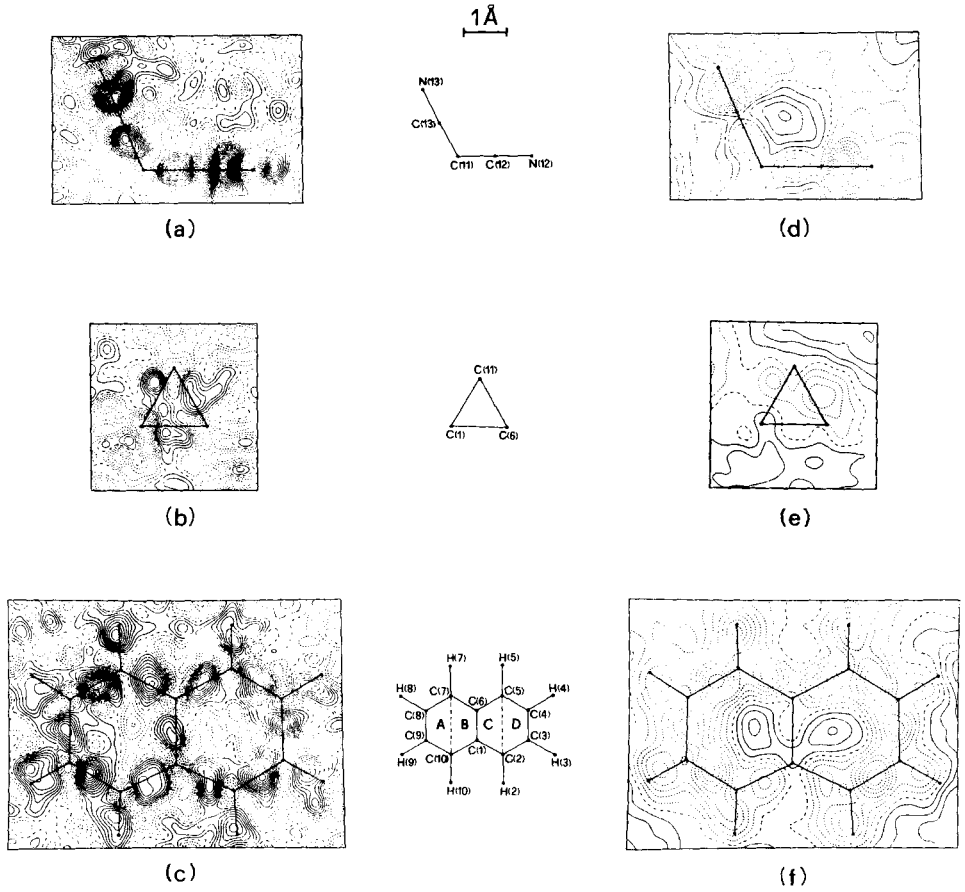

Figure. *Electrostatic deformation maps from multipole refinement.*

(*a*), (*b*), (*c*) Observed deformation density maps (large dashed lines are lines of zero density, solid contours are 0.05 eÅ^{-3}, short dashed lines are −0.05 eÅ^{-3}); (*d*), (*e*), (*f*) deformation electrostatic potential maps (contour are at interval of 0.05 eÅ^{-1}, solid lines are electropositive small dashed lines are electronegative).

(*a*), (*d*) Planes of the cyclopropane ring; (*b*), (*e*) planes through C(11), C(12), C(13), N(12) and N(13); (*c*), (*f*) compositions of the four maps corresponding to the least-squares planes C(2), C(3), C(4), C(5), **(D)**; C(1), C(2), C(5), C(6), (C); C(1), C(6), C(7), C(10), **(B)**, and C(7), C(8), C(9), C(10), **(A)**.

Table 1. *Summary of Least-Squares Refinements*

	All-data free-atom	High-order free-atom	Multipole refinement
R[%][a])[b])	6.07	9.53	5.08
R_w[%][c])[b])	4.19	5.96	3.11
G.o.f.[b])[d])	1.41	1.06	1.10
Number of observed (N)	3120	1567	3120
Number of variables (p)	169	136	417
Scale factor	5.52	5.40	5.37

[a]) $R = \Sigma||F_o|-k|F_c||/\Sigma|F_o|$.
[b]) From the *Valray* program.
[c]) $R_w = [\Sigma w(|F_o|-k|F_c|)^2/\Sigma w|F_o|^2]^{1/2}$.
[d]) G.o.f. $= [\Sigma w(|F_o|^2-k^2|F_c|^2)^2/(N-p)]^{1/2}$.

It is well known that the positional and especially the thermal parameters derived by means of a conventional refinement may be biased by bonding features for which the spherical atom model does not account. A way to overcome this bias is to determine positional and thermal parameters from reflections at high values of $\sin\theta/\lambda$ (high-order refinement) where the influence of bonding effects should be minimal. Several high-order refinements with increasing values of the $\sin\theta/\lambda$ threshold values revealed that bonding effects become negligible at $\sin\theta/\lambda = 0.70$ Å^{-1} and beyond.

An alternative procedure for avoiding bias in the refined parameters is to use in the refinement the atomic multipole formalism as described by *Stewart* [7]. A multipole refinement was carried out with the program *Valray* [4]. Lacking the neutron information, we used the 'polarized facility' [8] of *Valray* to estimate the time-average proton position of H-atoms. Curves for monopole and dipole scattering factors were taken from the H_2-molecule [9]. For each heavy atom the multipole model consists of two monopoles, a dipole, a quadrupole and an octopole. The generalized scattering factors for the two monopoles are computed from the canonical *Hartree-Fock* orbitals tabulated by *Clementi* [5]. The radial function for the higher multipoles are single exponentials $r^n\exp(-\alpha r)$ with n = 2,2,3 for dipole, quadrupole and octopole. Population parameters of inner monopoles (core density) were constrained to be equal for all heavy atoms. The heavy atoms were assigned first and second cumulant parameters; the H-atoms were given positional and isotropic thermal parameters. The scale factor is estimated by the sum of the monopole populations P_{p00} divided by $F(000)$. Details of various refinements are summarized in *Table 1*[1]). Corresponding interatomic distances and bond angles are shown in *Table 2*. Atomic numbering is defined in the *Figure*. Parallel calculations with 3363 reflections led to no significant improvement in the results.

Electrostatic Deformation Maps. – A number of difference *Fourier* maps, based on 3120 reflections, were calculated with the refined parameters of the multipole model, according to *Stewart* [10]. Residuals maps, based on $F_o(H)/k-F_c(H)$, represent electron density features that have not been described by the modeling functions. These maps

[1]) The atomic coordinates from the multipole model have been deposited at the *Cambridge Crystallographic Data Center*. The temperature factors and the measured structure factors (including weights) are available upon request.

Table 2. *Molecular Geometry of DICN*

	All data	*High order*	*Multipole refinement*
Distances [Å]			
C(1)–C(2)	1.476(2)	1.479(2)	1.476(1)
C(1)–C(6)	1.545(2)	1.540(3)	1.542(1)
C(1)–C(10)	1.474(2)	1.477(2)	1.474(1)
C(1)–C(11)	1.560(2)	1.562(3)	1.561(1)
C(2)–C(3)	1.342(2)	1.346(3)	1.350(1)
C(3)–C(4)	1.452(2)	1.451(4)	1.452(1)
C(4)–C(5)	1.344(2)	1.348(3)	1.350(1)
C(5)–C(6)	1.473(2)	1.478(3)	1.473(1)
C(6)–C(7)	1.472(2)	1.471(3)	1.472(1)
C(6)–C(11)	1.572(2)	1.571(2)	1.574(1)
C(7)–C(8)	1.344(2)	1.356(4)	1.350(2)
C(8)–C(9)	1.451(2)	1.442(4)	1.452(2)
C(9)–C(10)	1.336(2)	1.345(3)	1.348(1)
C(11)–C(12)	1.437(2)	1.430(3)	1.431(1)
C(11)–C(13)	1.436(2)	1.426(3)	1.427(1)
C(12)–N(12)	1.146(2)	1.155(3)	1.155(1)
C(13)–N(13)	1.148(2)	1.158(3)	1.157(1)
C(2)–H(2)	0.97(2)	0.97(2)	1.02(1)
C(3)–H(3)	1.00(2)	1.00(2)	1.07(1)
C(4)–H(4)	1.00(2)	1.00(2)	1.09(1)
C(5)–H(5)	0.98(2)	0.98(2)	1.02(1)
C(7)–H(7)	0.97(2)	0.97(2)	1.04(1)
C(8)–H(8)	0.99(2)	0.99(2)	1.05(1)
C(9)–H(9)	0.97(2)	0.96(2)	1.03(1)
C(10)–H(10)	0.97(2)	0.97(2)	1.04(1)
Angles [°] from multipole refinement			
C(2)–C(1)–C(6)	116.61(7)	C(1)–C(11)–C(13)	119.48(8)
C(2)–C(1)–C(10)	118.18(7)	C(6)–C(11)–C(12)	118.55(7)
C(2)–C(1)–C(11)	115.81(7)	C(6)–C(11)–C(13)	118.60(8)
C(6)–C(1)–C(10)	116.49(7)	C(12)–C(11)–C(13)	113.50(8)
C(6)–C(1)–C(11)	60.95(6)	C(11)–C(12)–N(12)	179.24(11)
C(10)–C(1)–C(11)	116.19(7)	C(11)–C(13)–N(13)	177.02(11)
C(1)–C(2)–C(3)	121.33(8)	C(1)–C(2)–H(2)	119.7(5)
C(2)–C(3)–C(4)	121.89(8)	C(3)–C(2)–H(2)	119.0(5)
C(3)–C(4)–C(5)	121.38(9)	C(2)–C(3)–H(3)	117.4(8)
C(4)–C(5)–C(6)	121.58(10)	C(4)–C(3)–H(3)	120.6(8)
C(1)–C(6)–C(5)	116.86(8)	C(3)–C(4)–H(4)	120.1(7)
C(1)–C(6)–C(7)	116.91(8)	C(5)–C(4)–H(4)	118.4(7)
C(1)–C(6)–C(11)	60.13(6)	C(4)–C(5)–H(5)	122.6(6)
C(5)–C(6)–C(7)	118.08(8)	C(6)–C(5)–H(5)	115.8(6)
C(5)–C(6)–C(11)	115.69(8)	C(6)–C(7)–H(7)	117.7(6)
C(7)–C(6)–C(11)	116.24(8)	C(8)–C(7)–H(7)	120.8(6)
C(6)–C(7)–C(8)	121.55(10)	C(7)–C(8)–H(8)	117.0(8)
C(7)–C(8)–C(9)	121.53(9)	C(9)–C(8)–H(8)	121.4(8)
C(8)–C(9)–C(10)	121.66(10)	C(8)–C(9)–H(9)	118.0(7)
C(1)–C(10)–C(9)	121.71(9)	C(10)–C(9)–H(9)	119.9(7)
C(1)–C(11)–C(6)	58.92(8)	C(1)–C(10)–H(10)	116.4(6)
C(1)–C(11)–C(12)	117.43(8)	C(9)–C(10)–H(10)	121.8(6)

Table 3. *Values of* $\langle w(|F_o|^2 - k^2|F_c|^2)^2\rangle$ *and Weighted Discrepancy Indices for Different Ranges of* $\sin\theta/\lambda$ *from Multipole Refinement*

Interval of $\sin\theta/\lambda$ [Å^{-1}]	$\langle w(\|F_o\|^2 - k^2\|F_c\|^2)^2\rangle$	R_w [%]	Number of reflections
0 –0.4270	1.13	1.5	387
0.4270–0.5380	0.90	2.6	354
0.5380–0.6159	0.94	3.3	333
0.6159–0.6779	1.06	4.2	341
0.6779–0.7302	1.09	4.5	330
0.7302–0.7760	1.00	5.3	305
0.7760–0.8169	1.06	5.8	313
0.8169–0.8541	1.09	6.9	318
0.8541–0.8883	1.10	8.0	307
0.8883–0.9200	1.13	11.3	132

for DICN show no indication of significant residual density. The residual values are between ± 0.20 eÅ^{-3}. These rather large extrema in the residual density maps are reflected in the relatively large R-factors in *Table 1*. The large values of R and R_w may be attributed to the systematic error in the high-angle intensities, to the large number of weak reflections in the data set and to icing on the crystal during data acquisition. In *Table 3* we report the averages of $w(|F_o|^2-k^2|F_c|^2)^2$ and weighted R-indices as a function of $\sin\theta/\lambda$. The numerical values of these quantities indicate the modest accuracy of the data. The deformation maps can guide us in assessing only qualitative information about the chemical bonding in the DICN molecule. The average standard deviation of the total density which is representative of the error in the deformation density at positions away from the atoms is estimated to be 0.08 eÅ^{-3}. The observed deformation density maps for DICN, based on $F_o(H)/k-F_c^{IAM}(H)$ (IAM = independent atom model and $F_o(H)$ are the observed structure factors with phases taken from the multipole model), are shown in the *Figure* (*a*, *b* and *c*). They have density accumulation in all bonds and in the lone-pair regions of the two cyano N-atoms. The triple bonds C(12)≡N(12) and C(13)≡N(13) appear to be polarized towards the corresponding N-atom. The broaded bond peaks in the cyclopropane ring clearly confirm the existence of a bond between C(1) and C(6). We also note that the peak height in this bond is smaller compared to the remaining ones of DICN molecule. The sequence of more and less pronounced bond peaks along the annulene ring correlates well with the systematic succession of long and short bond distances (see *Table 2*).

The deformation potential is computed with the sum:

$$\Delta\bar{\Phi}(x) = (4\pi V)^{-1}\Sigma_H \Delta F_H(e^{-2\pi i H\cdot x})/(\sin\theta/\lambda)^2$$

where $|H| = 2\sin\theta/\lambda$, λ is the X-ray wavelength and 2θ is the *Bragg* diffraction angle, $\Delta F_H = F_c^{IAM}(H)-F_o(H)/k$. The features of the deformation potential, shown in the *Figure* (*d*, *e* and *f*), are in qualitative agreement with those of similar deformation density maps. The deformation potential have negative holes on the backside of N-atoms which may be associated with lone-pair regions. Marked electronegative values with a minimum of -0.50 eÅ^{-1} are in the midpoint region of the triple bonds. In the cyclopropane ring, the electronegative and the zero-potential zone is distributed along the region with an extremum of -0.15 eÅ^{-1} located between C(6) and C(11). Along the annulene system the deformation potential is more markedly electronegative in the short bond regions.

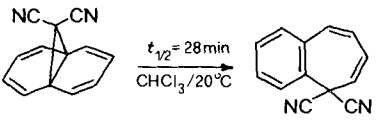

Discussion. – In *Table 1*, the *R*-factors are much lower for the multipole refinement, indicating that a significant fraction of the disagreement between observed and calculated structure factors in the conventional refinement may be attributed to deficiences for the valence electron distribution. Interatomic distances from conventional, high-order and multipole refinement parameters are compared in *Table 2*. As expected the effect of the aspherical electron distribution on the conventional refinement result is largest for H-positions. The resulting C–H bond distances are 0.04–0.09 Å shorter than those determined from polarized H-atom refinement. Comparison of the bond distances from various refinements indicates that, except for hydrogen, the asphericity shifts are quite small. However, the largest asphericity shift is found for C(9)–C(10) which is 0.012 Å longer for the multipole refinement than in the conventional refinement. Furthermore, we note that the two triple bonds are, on the average, 0.009 Å shorter in the conventional refinement. Also, the multipole refinement is in closer agreement with that of the high-order refinement. It appears from this study that the multipole model leads to a good qualitative determination of the electrostatic deformation properties in DICN crystals. In the deformation density map of the *Figure* (*c*) a bonding maximum between C(1) and C(6) atom is evident. In addition the deformation potential (see *Figure* (*f*)) indicates a bonding interaction for the above atoms, that is another evidence of the closure of the cyclopropane ring. Also, the C(1)–C(6) bond in the three-membered ring (see *Figure* (*b* and *e*)) appears to be somewhat weaker than other bonds of DICN molecule. This observation is reinforced by the following isomerization process [11] of DICN molecule at room temperature showing that the three-membered ring is the most reactive region of the molecule. Finally, the trends of the deformation density and potential along the annulene ring (see *Figure* (*c* and *f*)) clearly show the bisnorcaradienic electronic structure of DICN molecule.

REFERENCES

[1] *T. Pilati & M. Simonetta*, Acta Crystallogr., Sect. B *32*, 1912 (1976).
[2] *R. Bianchi, T. Pilati & M. Simonetta*, Acta Crystallogr., Sect. C *39*, 378 (1983).
[3] *P. Becker & P. Coppens*, Acta Crystallogr., Sect. A *30*, 148 (1974).
[4] *R.F. Stewart*, Valray System, Private Communication (1981).
[5] *E. Clementi*, Tables of atomic functions, Supplement to IBM J. Res. Dev. 9:2 (1965).
[6] *W.J. Hehre, R.F. Stewart & J.A. Pople*, J. Chem. Phys. *51*, 2657 (1969).
[7] *R.F. Stewart*, Acta Crystallogr., Sect. A *32*, 565 (1976).
[8] *A.F.J. Ruysink & R.F. Stewart*, A.C.A., Summer meeting, 14–16 August 1974, University Park, Pennsylvania, paper D7.
[9] *R.F. Stewart, J. Bentley & B. Goodman*, J. Chem. Phys. *63*, 3786 (1975).
[10] *R.F. Stewart*, Chem. Phys. Lett. *65*, 335 (1979).
[11] *E. Vogel, T. Scholl, J. Lex & G. Hohlneicher*, Angew. Chem. Int. Ed. *21*, 869 (1982).